Inorganica Chimica Acta 387 (2012) 338–345

Contents lists available at SciVerse ScienceDirect

Inorganica Chimica Acta

journal homepage: www.elsevier.com/locate/ica

(Ethynylferrocenyl)phosphine ruthenium complexes in catalytic β-oxopropyl benzoate formation

Bianca Milde, Tobias Rüffer, Heinrich Lang *

Chemnitz University of Technology, Faculty of Science, Institute of Chemistry, Department of Inorganic Chemistry, Straße der Nationen 62, 09111 Chemnitz, Germany

ARTICLE INFO

Article history:
Received 28 November 2011
Received in revised form 8 February 2012
Accepted 15 February 2012
Available online 23 February 2012

Keywords:
(Ethynylferrocenyl)phosphine
β-Oxopropyl esters
Ruthenium
Ferrocene
Catalysis

ABSTRACT

The synthesis of a series of (ethynylferrocenyl)phosphino ruthenium compounds of type (FcC≡C)R_2-P($RuCl_2(\eta^6$-*p*-cymene)) (**3a**, R = C_6H_5; **3b**, R = 2-$CH_3C_6H_4$; **3c**, R = $^cC_4H_3O$; **3d**, R = *t*-Bu; **3e**, R = $^cC_6H_{11}$; *p*-cymene = 1-$^iC_3H_7$-4-CH_3-C_6H_4; Fc = Fe(η^5-C_5H_4)(η^5-C_5H_5)) and ($RuCl_2(\eta^6$-*p*-cymene))(FcC≡C)P(C≡CP-$Ph_2(RuCl_2(\eta^6$-*p*-cymene)))$_2$ (**10**) resulting from the addition of ferrocenylphosphines P(C≡CFc)R_2 (**1a**–**1e**) or P(C≡CFc)(C≡C$PPh_2)_2$ (**9**) to $[RuCl_2(\eta^6$-*p*-cymene)$]_2$ (**2**) is described. The structures of **3b**, **3c** and **10** in the solid state are reported confirming the expected tetrahedral coordination sphere about the phosphorus atom as well as the "piano-stool" arrangement about the ruthenium atom(s). Ruthenium complexes **3** and **10** are catalytically active under mild conditions in the alkyne-to-carboxylic acid coupling as it was shown for the reaction of propargyl alcohol with benzoic acid. A comparison with literature known $[RuCl_2(PR_3)(\eta^6$-*p*-cymene)] catalysts is presented.

1. Introduction

Since the pioneering work of Dixneuf and co-workers [1a], the ruthenium-promoted synthesis of β-oxo esters developed rapidly and is now-a-days an integral part in homogeneous catalysis, applicable on bulky or functionalized carboxylic acids [2]. This reaction is atom-economic, which provides an elegant alternative to classical synthesis methodologies of β-oxo esters. Established standard methods for the preparation of β-oxo esters include, for example, the preparation from propargylic alcohols by hydration-esterification steps [3–6] or the carboxylation of α-halo ketones [6–13]. In general, β-oxo esters are of versatile interest in organic synthesis and industry, because they easily form α-hydroxy ketones which are structural building blocks in, for example, the synthesis of natural products [3–6], antibacterial compounds [14] and intermediates for furanones and imidazoles, respectively [1a,14]. In addition, β-oxo esters can be used as photolabile protecting groups for carboxylic acids [6,15] or even as activated esters for peptide synthesis [14]. Early works on the catalytic addition of terminal alkynes to carboxylic acids include the application of $[Ru_3(CO)_{12}]$ [1,16] or $[RuCl_3 \times 3H_2O]$ [1a] as catalyst precursors. In recent years, several phosphine-carrying catalysts have been developed, for example, $[RuCl_2(\eta^6$-*p*-cymene)$(PR_3)]$ (R = Ph, Me, OPh) [1,17] or $[Ru(\mu O_2CH)(CO)_2(PPh_3)]_2$ [1b,2], which show high conversions and regioselectivity under mild reaction conditions using basic phosphines. In contrast, Goossen et al. reported that even better yields are obtained using phosphines with strong π-acceptor ability, e.g. P($^cC_4H_3O)_3$ [9]. In addition, also water-soluble [3,35] or on MCM-41-immobilized ruthenium(II) [19] catalysts have been developed.

We here report on the synthesis of diverse (ethynylferrocenyl)phosphino ruthenium(II) complexes and their application in the catalytic formation of β-oxopropyl benzoate to clarify the question whether strong or weak electron donating groups at the phosphorus atom are responsible for the activity. Given the fact that PR_3 groups are known to be highly sensitive toward oxygen we introduced a ferrocenyl group for more stability and an additional alkynyl functionality due to its electron-withdrawing nature. Also, the preparation of a molecule featuring three ruthenium dichloro *p*-cymene units is discussed to evaluate possible synergistic and cooperative effects in the catalytic performance.

2. Experimental

2.1. General procedure and materials

All reactions were performed under an atmosphere of nitrogen using standard Schlenk techniques. Diethyl ether and dichloromethane were dried over sodium/benzophenone and calcium hydride, respectively, and purified by distillation. For filtrations Celite (purified and annealed, Erg. B.6, Riedel de Haen) was used. Column chromatographies were performed using silica with a particle size of 40–60 μm (230–400 mesh (ASTM), Becker). Compounds Fc–C≡C–PR_2 (**1a**–**1e**) [20,21], HC≡C–PPh_2 (**4**) [22], $P(NEt_2)Cl_2$ (**5**) [23] and $[RuCl_2(\eta^6$-*p*-cymene$)]_2$ (**7**) [24] were

* Corresponding author. Tel.: +49 (0)371 531 21210; fax: +49 (0)371 531 21219.
E-mail address: heinrich.lang@chemie.tu-chemnitz.de (H. Lang).

0020-1693/$ - see front matter © 2012 Elsevier B.V. All rights reserved.
doi:10.1016/j.ica.2012.02.025

synthesized according to published procedures. All other chemicals were obtained from commercial suppliers and used without further purification.

The ^{1}H NMR spectra were recorded with a Bruker Avance III 500 spectrometer working at 500.3 MHz. The $^{13}C\{^1H\}$ and $^{31}P\{^1H\}$ NMR spectra were recorded at 125.7 MHz and 202.5 MHz, respectively. Chemical shifts are reported in δ units (parts per million) downfield from tetramethylsilane with the solvent as reference signal (^{1}H NMR: standard internal $CDCl_3$, δ 7.26; $^{13}C\{^1H\}$ NMR: standard internal $CDCl_3$, δ 77.16; $^{31}P\{^1H\}$ NMR: standard external rel. 85% H_3PO_4, δ 0.0 and $P(OMe)_3$, δ 139.0). High resolution mass spectra were recorded with a Bruker Daltonik micrOTOF-QII spectrometer (ESI-TOF). Elemental analyses were carried out with a Thermo FlashAE 1112 series instrument. Melting points of analytical pure samples were determined by a Gallenkamp MFB 595 010 M melting point apparatus. FT IR spectra were recorded with a Thermo Nicolet IR 200 spectrometer using either KBr pellets or NaCl plates.

2.2. General procedure for the synthesis of ruthenium complexes **3a**–**3e** and **10**

0.5 g of **1** or **9** and 0.5 or 1.5 equiv. of $[RuCl_2(\eta^6\text{-}p\text{-cymene})]_2$ (**2**) were dissolved in 40 mL of dry dichloromethane. The solution was stirred for 2 h at ambient temperature. Afterwards, the solvent was removed in vacuum and the residue was washed 5–6 times with 5 mL portions of diethyl ether. After drying in vacuum the appropriate complexes were obtained as orange solids.

2.2.1. Synthesis of (FcC≡C)(C_6H_5)$_2$P(RuCl$_2$(η^6-p-cymene)) (**3a**)

Following the synthesis methodology described above, 0.5 g (1.27 mmol) of **1a** were reacted with 0.39 g (0.63 mmol) of **2**. After appropriate work-up, **3a** was isolated as an air stable orange solid. Yield: 0.88 g (1.22 mmol, 97% based on **2**). *Anal.* Calc. for $C_{34}H_{33}Cl_2FePRu \times 1/4\ CH_2Cl_2$ (721.65 g/mol): C, 57.00; H, 4.68. Found: C, 56.96; H, 4.66%. Mp.: 200 °C (dec.). IR (KBr, ν/cm^{-1}): 1436 (m, P–C), 2153 (m, C≡C). ^{1}H NMR (500.30 MHz, $CDCl_3$, δ): 1.23 (d, $^3J_{HH}$ = 6.9 Hz, 6H, CH(CH_3)$_2$), 2.00 (s, 3H, CH_3), 2.95 (sept, $^3J_{HH}$ = 7.0 Hz, 1H, CH(CH$_3$)$_2$), 4.30 (s, 5H, C_5H_5), 4.37 (pt, $^3J_{HH}$ = 1.9 Hz, 2H, C_5H_4), 4.62 (pt, $^3J_{HH}$ = 1.9 Hz, 2H, C_5H_4), 5.23–5.26 (m, 2H, C_6H_4), 5.30 (s, CH_2Cl$_2$), 5.31–5.33 (m, 2H, C_6H_4), 7.33–7.39 (m, 6H, H^{m,p}/C_6H_5), 8.01–8.09 (m, 4H, H^o/C_6H_5). $^{13}C\{^1H\}$ NMR (125.81 MHz, $CDCl_3$, δ): 17.7 (s, CH_3), 22.2 (s, CH(CH_3)$_2$), 30.5 (s, CH(CH$_3$)$_2$), 53.57 (s, CH_2Cl$_2$), 62.1 (d, $^3J_{CP}$ = 3.0 Hz, C^i/C_5H_4), 70.1 (s, C$^\beta$/C_5H_4), 70.4 (s, C_5H_5), 72.4 (d, $^4J_{CP}$ = 1.0 Hz, C$^\alpha$/C_5H_4), 78.3 (d, $^1J_{CP}$ = 53.3 Hz, C≡C–P), 86.8 (d, $^2J_{CP}$ = 6.2 Hz, C_6H_4), 90.6 (d, $^2J_{CP}$ = 4.3 Hz, C_6H_4), 96.0 (s, C^i/C_6H_4), 109.6 (s, C^i/C_6H_4), 110.4 (d, $^2J_{CP}$ = 13.4 Hz, C≡C–P), 128.1 (d, $^3J_{CP}$ = 10.8 Hz, C^m/C_6H_5), 130.4 (d, $^4J_{CP}$ = 2.7 Hz, C^p/C_6H_5), 132.7 (d, $^1J_{CP}$ = 54.2 Hz, C^i/C_6H_5), 133.3 (d, $^2J_{CP}$ = 10.3 Hz, C^o/C_6H_5). $^{31}P\{^1H\}$ NMR (202.53 MHz, $CDCl_3$, δ): −3.3. HRMS (ESI-TOF) $C_{34}H_{33}Cl_2FePRu$ [M+nK]$^+$ m/z: calcd.: 740.9717, found: 740.9639; [M−Cl]$^+$ m/z: calcd.: 665.0404, found: 665.0448.

2.2.2. Synthesis of (FcC≡C)(2-CH$_3$C$_6$H$_4$)$_2$P(RuCl$_2$(η^6-p-cymene)) (**3b**)

0.5 g (1.18 mmol) of **1b** were reacted with 0.36 g (0.59 mmol) of **2**. After appropriate work-up, complex **3b** was isolated as orange solid. Yield: 0.71 g (0.97 mmol, 82% based on **2**). *Anal.* Calc. for $C_{36}H_{37}Cl_2FePRu$ (728.47 g/mol): C, 59.35; H, 5.12. Found: C, 59.42; H, 5.13%. Mp.: 195 °C. IR (KBr, ν/cm^{-1}): 1468 (m, P–C), 2150 (s, C≡C). ^{1}H NMR (500.30 MHz, $CDCl_3$, δ): 1.08 (d, $^3J_{HH}$ = 7.0 Hz, 6H, CH(CH_3)$_2$), 2.10 (s, 3H, CH_3), 2.16 (s, 6H, 2-CH_3C$_6$H$_4$), 2.86 (sept, $^3J_{HH}$ = 7.0 Hz, 1H, CH(CH$_3$)$_2$), 4.18 (s, 5H, C_5H_5), 4.30 (pt, $^3J_{HH}$ = 1.9 Hz, 2H, C_5H_4), 4.52 (pt, $^3J_{HH}$ = 1.9 Hz, 2H, C_5H_4), 5.04–5.07 (m, 2H, C_6H_4), 5.31–5.34 (m, 2H, C_6H_4), 7.09–7.14 (m, 2H, H^p/2-CH$_3$C$_6$H$_4$), 7.29–7.35 (m, 4H, H^m/2-CH$_3$C$_6$H$_4$), 8.43–8.52 (m, 2H, H^o/2-CH$_3$C$_6$H$_4$). $^{13}C\{^1H\}$ NMR (125.81 MHz, $CDCl_3$, δ): 17.5 (s, CH_3), 21.8 (s, CH(CH_3)$_2$), 22.5 (d, $^3J_{CP}$ = 4.9 Hz, 2-CH_3C$_6$H$_4$), 30.0 (s, CH(CH$_3$)$_2$), 62.7 (d, $^3J_{CP}$ = 3.4 Hz, C^i/C_5H_4), 69.9 (s, C$^\beta$/C_5H_4), 70.3 (s, C_5H_5), 72.1 (d, $^4J_{CP}$ = 0.6 Hz, C$^\alpha$/C_5H_4), 79.6 (C≡C–P*)), 86.6 (d, $^2J_{CP}$ = 5.3 Hz, C_6H_4), 91.5 (d, $^2J_{CP}$ = 5.1 Hz, C_6H_4), 95.2 (s, C^i/C_6H_4), 109.5 (d, $^2J_{CP}$ = 13.5 Hz, C≡C–P), 109.6 (s, C^i/C_6H_4), 125.7 (d, J_{CP} = 12.5 Hz, 2-CH$_3$C$_6$H$_4$), 130.4 (d, J_{CP} = 16.7 Hz, 2-CH$_3$C$_6$H$_4$), 130.9 (d, J_{CP} = 2.4 Hz, 2-CH$_3$C$_6$H$_4$), 131.8 (d, J_{CP} = 7.9 Hz, 2-CH$_3$C$_6$H$_4$), 135.4 (m, 2-CH$_3$C$_6$H$_4$), 141.9 (d, J_{CP} = 5.9 Hz, 2-CH$_3$C$_6$H$_4$). $^{31}P\{^1H\}$ NMR (202.53 MHz, $CDCl_3$, δ): −9.1. HRMS (ESI-TOF) $C_{36}H_{37}Cl_2FePRu$ [M]$^+$ m/z: calcd.: 728.0403, found: 728.0413; [M−Cl]$^+$ m/z: calcd.: 693.0717, found: 693.0709. *) Signal concealed by $CDCl_3$.

2.2.3. Synthesis of (FcC≡C)(^{c}C$_4$H$_3$O)$_2$P(RuCl$_2$(η^6-p-cymene)) (**3c**)

0.5 g (1.34 mmol) of **1c** were reacted with 0.41 g (0.67 mmol) of **2**. After appropriate work-up, **3c** was isolated as an orange solid. Yield: 0.88 g (1.26 mmol, 94% based on **2**). *Anal.* Calc. for $C_{30}H_{29}Cl_2FeO_2PRu \times 1/5\ CH_2Cl_2$ (697.33 g/mol): C, 52.02; H, 4.25. Found: C, 52.03; H, 4.49%. Mp.: 175 °C. IR (KBr, ν/cm^{-1}): 1007 (s, C–O), 1458 (w, P–C), 2159 (s, C≡C). ^{1}H NMR (500.30 MHz, $CDCl_3$, δ): 1.18 (d, $^3J_{HH}$ = 6.9 Hz, 6H, CH(CH_3)$_2$), 2.06 (s, 3H, CH$_3$), 2.91 (sept, $^3J_{HH}$ = 6.9 Hz, 1H, CH(CH$_3$)$_2$), 4.27 (s, 5H, C_5H_5), 4.31 (pt, $^3J_{HH}$ = 1.9 Hz, 2H, C_5H_4), 4.58 (pt, $^3J_{HH}$ = 1.9 Hz, 2H, C_5H_4), 5.30 (s, CH_2Cl$_2$), 5.49–5.51 (m, 2H, C_6H_4), 5.54–5.57 (m, 2H, C_6H_4), 6.48 (dt, $^4J_{HP}$ = 1.6 Hz, $^3J_{HH}$ = 3.4 Hz, $^3J_{HH}$ = 1.6 Hz, 2H, H^4/C_4H_3O), 7.21 (m, 2H, H^3/C_4H_3O), 7.68 (m, 2H, H^5/C_4H_3O). $^{13}C\{^1H\}$ NMR (125.81 MHz, $CDCl_3$, δ): 17.8 (s, CH_3), 22.0 (s, CH(CH_3)$_2$), 30.4 (s, CH(CH$_3$)$_2$), 53.53 (s, CH_2Cl$_2$), 61.7 (d, $^3J_{CP}$ = 3.7 Hz, C^i/C_5H_4), 70.1 (s, C$^\beta$/C_5H_4), 70.7 (s, C_5H_5), 72.5 (d, $^4J_{CP}$ = 0.8 Hz, C$_\alpha$/C_5H_4), 74.0 (d, $^1J_{CP}$ = 112.6 Hz, C≡C–P), 86.9 (d, $^2J_{CP}$ = 6.7 Hz, C_6H_4), 90.9 (d, $^2J_{CP}$ = 5.4 Hz, C_6H_4), 96.7 (s, C^i/C_6H_4), 109.0 (d, $^2J_{CP}$ = 18.1 Hz, C≡C–P), 109.5 (s, C^i/C_6H_4), 111.6 (d, $^3J_{CP}$ = 7.6 Hz, C^4/C_4H_3O), 123.0 (d, $^2J_{CP}$ = 17.7 Hz, C^3/C_4H_3O), 144.5 (d, $^1J_{CP}$ = 81.0 Hz, C^2/C_4H_3O), 147.4 (d, $^4J_{CP}$ = 5.6 Hz, C^5/C_4H_3O). $^{31}P\{^1H\}$ NMR (202.53 MHz, $CDCl_3$, δ): −26.0. HRMS (ESI-TOF) $C_{30}H_{29}Cl_2FeO_2PRu$ [M]$^+$ m/z: calcd.: 679.9674, found: 679.9673.

2.2.4. Synthesis of (FcC≡C)(^{t}Bu)$_2$P(RuCl$_2$(η^6-p-cymene)) (**3d**)

Reaction of 0.5 g (1.41 mmol) of **1d** with 0.42 g (0.69 mmol) of **2** gave, after appropriate work-up, complex **3d** which was isolated as an air stable orange solid. Yield: 0.87 g (1.28 mmol, 93% based on **2**). *Anal.* Calc. for $C_{30}H_{41}Cl_2FePRu \times 1/4\ CH_2Cl_2$ (681.68 g/mol): C, 53.30; H, 6.14. Found: C, 53.26; H, 6.22%. Mp.: 151 °C (dec.). IR (KBr, ν/cm^{-1}): 1467 (w, P–C), 2158 (s, C≡C), 2959 (s, C–H). ^{1}H NMR (500.30 MHz, $CDCl_3$, δ): 1.30 (d, $^3J_{HH}$ = 6.9 Hz, 6H, CH(CH_3)$_2$), 1.51 (d, $^3J_{HP}$ = 14.8 Hz, 18H, C(CH_3)$_3$), 2.15 (s, 3H, CH_3), 3.12 (sept, $^3J_{HH}$ = 6.5 Hz, 1H, CH(CH$_3$)$_2$), 4.31 (s, 5H, C_5H_5), 4.37 (m, 2H, C_5H_4), 4.57 (m, 2H, C_5H_4), 5.30 (s, CH_2Cl$_2$), 5.40–5.48 (m, 4H, C_6H_4). $^{13}C\{^1H\}$ NMR (125.81 MHz, $CDCl_3$, δ): 17.7 (s, CH_3), 22.2 (s, CH(CH_3)$_2$), 29.5 (s, CH(CH$_3$)$_2$), 30.6 (d, $^2J_{CP}$ = 3.5 Hz, C(CH_3)$_3$), 39.3 (d, $^1J_{CP}$ = 14.8 Hz, C(CH$_3$)$_3$), 53.52 (s, CH$_2$Cl$_2$), 62.8 (d, $^3J_{CP}$ = 2.3 Hz, C^i/C_5H_4), 69.9 (s, C_5H_4), 70.0 (s, C_5H_5), 72.0 (s, C_5H_4), 80.8 (d, $^1J_{CP}$ = 33.0 Hz, C≡C–P), 89.2 (d, $^2J_{CP}$ = 5.0 Hz, C_6H_4), 89.3 (d, $^2J_{CP}$ = 4.6 Hz, C_6H_4), 97.2 (s, C_6H_4), 106.5 (s, C_6H_4), 108.1 (d, $^2J_{CP}$ = 2.2 Hz, C≡C–P). $^{31}P\{^1H\}$ NMR (202.53 MHz, $CDCl_3$, δ): 26.7. HRMS (ESI-TOF) $C_{30}H_{41}Cl_2FePRu$ [M−Cl]$^+$ m/z: calcd.: 625.1029, found: 625.0936; [M−(η^6-p-cymen)RuCl$_2$]$^+$ m/z: calcd.: 354.1194, found: 354.1188.

2.2.5. Synthesis of (FcC≡C)(^{c}C$_6$H$_{11}$)$_2$P(RuCl$_2$(η^6-p-cymene)) (**3e**)

Reaction of 0.5 g (1.23 mmol) of **1e** with 0.38 g (0.62 mmol) of **2** gave, after appropriate work-up, **3e** which was isolated as an orange solid. Yield: 0.86 g (1.17 mmol, 94% based on **2**). *Anal.* Calc. for $C_{34}H_{45}Cl_2FePRu \times 1/4\ CH_2Cl_2$ (733.75 g/mol): C, 56.06; H, 6.25. Found: C, 56.37; H, 6.49%. Mp.: 201 °C. IR (KBr, ν/cm^{-1}): 1447 (m, P–C), 2154 (m, C≡C), 2924 (vs C–H). ^{1}H NMR

(500.30 MHz, $CDCl_3$, δ): 1.25 (d, $^3J_{HH}$ = 6.9 Hz, 6H, CH(CH_3)$_2$), 1.22–1.35 (m, 6H, C_6H_{11}), 1.54–1.69 (m, 6H, C_6H_{11}), 1.76–1.81 (m, 4H, C_6H_{11}), 1.90–1.94 (m, 2H, C_6H_{11}), 2.01–2.03 (m, 2H, C_6H_{11}), 2.11 (s, 3H, CH_3), 2.47–2.53 (m, 2H, H^1/C_6H_{11}), 3.02 (sept, $^3J_{HH}$ = 6.9 Hz, $CH(CH_3)_2$), 4.28 (s, 5H, C_5H_5), 4.36 (pt, $^3J_{HH}$ = 1.8 Hz, 2H, C_5H_4), 4.57 (pt, $^3J_{HH}$ = 1.8 Hz, 2H, C_5H_4), 5.29 (s, CH_2Cl_2), 5.39–5.42 (m, 4H, C_6H_4). $^{13}C\{^1H\}$ NMR (125.81 MHz, $CDCl_3$, δ): 17.7 (s, CH_3), 22.2 (s, CH(CH_3)$_2$), 26.2 (s, C_6H_{11}), 26.9 (d, J_{CP} = 11.0 Hz, C_6H_{11}), 27.3 (d, J_{CP} = 13.3 Hz, C_6H_{11}), 27.9 (d, J_{CP} = 4.0 Hz, C_6H_{11}), 28.7 (m, C_6H_{11}), 29.9 (s, $CH(CH_3)_2$), 34.3 (d, $^1J_{CP}$ = 26.4 Hz, C_1/C_6H_{11}), 53.55 (s, CH_2Cl_2), 62.8 (d, $^3J_{CP}$ = 2.7 Hz, C^i/C_5H_4), 69.9 (s, C_5H_4), 70.3 (s, C_5H_5), 72.3 (s, C_5H_4), 79.0 (d, $^1J_{CP}$ = 65.1 Hz, C≡C–P), 88.5 (d, $^2J_{CP}$ = 4.8 Hz, C_6H_4), 90.0 (d, $^2J_{CP}$ = 4.5 Hz, C_6H_4), 97.3 (s, C_6H_4), 105.1 (s, C_6H_4), 108.1 (d, $^2J_{CP}$ = 4.5 Hz, C≡C–P). $^{31}P\{^1H\}$ NMR (202.53 MHz, $CDCl_3$, δ): 14.4. HRMS (ESI-TOF) $C_{34}H_{45}Cl_2FePRu$ [M - Cl]$^+$ *m/z*: calcd.: 677.1343, found: 677.1249.

2.3. Synthesis of (Et$_2$N)P(C≡C–P(C$_6$H$_5$)$_2$)$_2$ (**6**)

Phosphine **6** was synthesized by a modified literature procedure. [22] To 2.0 g (9.52 mmol) of **4** dissolved in 50 mL of dry diethyl ether, 3.8 mL (9.5 mmol) of ^{n}BuLi were added dropwise at −50 °C. After stirring the solution for 30 min at ambient temperature it was again cooled to −30 °C and 0.69 mL (826 mg, 4.75 mmol) of Cl_2PNEt_2 (**5**) were added dropwise. The reaction mixture was stirred at ambient temperature for 1 h and then filtered through a pad of Celite. The resulting solution was evaporated to dryness and the product was obtained as brown viscous oil in high purity. Phosphine **6** was used without further purification steps. Yield: 2.4 g (4.68 mmol, 97% based on **5**). $C_{32}H_{30}NP_3$ (521.51 g/mol). $^{31}P\{^1H\}$ NMR (101.249 MHz, $CDCl_3$, δ): −34.0 (d, $^3J_{PP}$ = 2.7 Hz, Ph_2P), −0.9 (t, $^3J_{PP}$ = 3.2 Hz, Et_2NP).

2.4. Synthesis of P(C≡CFc)(C≡CPPh$_2$)$_2$ (**9**)

To a solution of 2.4 g (4.68 mmol) of **6** in 50 mL of dry diethyl ether, 10 mL of a 1.0 M solution of HCl (2 equiv.) in diethyl ether were added slowly at ambient temperature. The resulting mixture was stirred for 1 h and then added dropwise to a cooled solution (−50 °C) of **8** in dry diethyl ether. Compound **8** was prepared by dropwise addition of 1.7 mL (4.25 mmol) of ^{n}BuLi to a solution of 0.89 g (4.26 mmol) of ethynyl ferrocene in 30 mL of dry diethyl ether. The resulting mixture was stirred for 1 h at ambient temperature and was then concentrated in vacuum. The residue was purified by column chromatography on silica gel (column size: 4 × 20 cm) using *n*-hexane as eluent. Phosphine **9** was obtained as a red solid. Yield: 1.63 g (2.48 mmol, 58% based on ^{n}BuLi). *Anal.* Calc. for $C_{40}H_{29}FeP_3$ (658.42 g/mol): C, 72.97; H, 4.44. Found: C, 73.33; H, 4.62%. IR (NaCl, ν/cm^{-1}): 1434 (m, P–C), 2151 (s, C≡C), 2175 (m, C≡C). ^1H NMR (250.130 MHz, $CDCl_3$, δ): 4.26 (s, 5H, C_5H_5), 4.30 (pt, $^3J_{HH}$ = 1.9 Hz, 2H, C_5H_4), 4.57 (pt, $^3J_{HH}$ = 1.9 Hz, C_5H_4), 7.32–7.40 (m, 12H, H^{m,p}/C_6H_5), 7.63–7.71 (m, 8 H, H^o/C_6H_5). $^{13}C\{^1H\}$ NMR (62.895 MHz, $CDCl_3$, δ): 62.8 (d, $^3J_{CP}$ = 0.5 Hz, C^i/C_5H_4), 69.8 (s, C$^\beta$/C_5H_4), 70.4 (s, C_5H_5), 72.4 (d, $^4J_{CP}$ = 1.8 Hz, C$^\alpha$/C_5H_4), 74.1 (dpt, $^1J_{CP}$ = 13.4 Hz, $^4J_{CP}$ = 2.3 Hz, FcC≡CP), 99.7 (dpt, $^1J_{CP}$ = 3.8 Hz, $^2J_{CP}$ = 2.3 Hz, Ph_2PC≡C), 105.6 (dd, $^1J_{CP}$ = 19.1 Hz, $^2J_{CP}$ = 4.2 Hz, Ph_2PC≡C), 107.5 (d, $^2J_{CP}$ = 13.7 Hz, FcC≡CP), 128.9 (d, $^3J_{CP}$ = 7.8 Hz, C^m/C_6H_5), 129.4 (s, C^p/C_6H_5), 132.9 (d, $^2J_{CP}$ = 20.6 Hz, C^o/C_6H_5), 135.1 (d, $^1J_{CP}$ = 6.2 Hz, $^4J_{CP}$ = 1.0 Hz, C^i/C_6H_5). $^{31}P\{^1H\}$ NMR (101.249 MHz, $CDCl_3$, δ): −88.2 (t, $^3J_{PP}$ = 4.8 Hz, FcC≡CP), −32.7 (d, $^3J_{PP}$ = 4.8 Hz, Ph_2PC≡C). HRMS (ESI-TOF) $C_{40}H_{29}FeP_3$ [M]$^+$ *m/z*: calcd.: 658.0827, found: 658.0778.

2.5. Synthesis of (RuCl$_2$(η^6-*p*-cymene))(FcC≡C)P(C≡CPPh$_2$(RuCl$_2$(η^6-*p*-cymene)))$_2$ (**10**)

0.5 g (0.76 mmol) of **9** were reacted with 0.70 g (1.14 mmol) of **2**. After appropriate work-up (Section 2.2), **10** was isolated as an orange solid. Yield: 1.18 g (0.75 mmol, 99% based on **9**). *Anal.* Calc. for $C_{70}H_{71}Cl_6FeP_3Ru_3$ (1577.01 g/mol): C, 53.31; H, 4.54. Found: C, 53.05; H, 4.45%. Mp.: 150 °C. IR (NaCl, ν/cm^{-1}): 1435 (m, P–C), 2155 (m, C≡C), 2179 (m, C≡C). ^1H NMR (250.130 MHz, $CDCl_3$, δ): 0.98 (d, $^3J_{HH}$ = 4.5 Hz, 6H, CH(CH_3)$_2$), 1.00 (d, $^3J_{HH}$ = 4.5 Hz, 6H, CH(CH_3)$_2$), 1.23 (d, $^3J_{HH}$ = 6.0 Hz, 6H, CH(CH_3)$_2$), 1.81 (s, 6H, CH_3), 2.00 (s, 3H, CH_3), 2.55 (sept, $^3J_{HH}$ = 6.9 Hz, 2H, $CH(CH_3)_2$), 2.88 (sept, $^3J_{HH}$ = 6.9 Hz, 1H, $CH(CH_3)_2$), 4.23 (s, 5H, C_5H_5), 4.36 (pt, $^3J_{HH}$ = 1.9 Hz, C_5H_4), 4.58 (pt, $^3J_{HH}$ = 1.9 Hz, C_5H_4), 5.22–5.25 (m, 2H, C_6H_4), 5.39–5.49 (m, 6H, C_6H_4), 5.56–5.58 (m, 2H, C_6H_4), 5.64–5.67 (m, 2H, C_6H_4), 7.27–7.31 (m, 6H, H^{m,p}/C_6H_5), 7.35–7.38 (m, 6H, H^{m,p}/C_6H_5), 8.01–8.09 (m, 8H, H^o/C_6H_5). $^{13}C\{^1H\}$ NMR (125.81 MHz, $CDCl_3$, δ): 17.6 (s, CH_3), 18.1 (s, CH_3), 21.7 (s, CH(CH_3)$_2$), 22.2 (s, CH(CH_3)$_2$), 22.3 (s, CH(CH_3)$_2$), 30.4 (s, $CH(CH_3)_2$), 30.8 (s, $CH(CH_3)_2$), 60.1 (d, $^3J_{CP}$ = 3.6 Hz, C^i/C_5H_4), 70.8 (s, C$^\beta$/C_5H_4), 70.9 (s, C_5H_5), 72.7 (m, C$^\alpha$/C_5H_4), 73.5 (d, $^1J_{CP}$ = 127.4 Hz, FcC≡CP), 86.4 (d, $^2J_{CP}$ = 5.4 Hz, C_6H_4), 87.3 (d, $^2J_{CP}$ = 6.0 Hz, C_6H_4), 88.0 (d, $^2J_{CP}$ = 6.2 Hz, C_6H_4), 89.9 (d, $^2J_{CP}$ = 7.0 Hz, C_6H_4), 90.0 (d, $^2J_{CP}$ = 4.3 Hz, C_6H_4), 91.4 (d, $^2J_{CP}$ = 5.0 Hz, C_6H_4), 97.1 (s, C^i/C_6H_4), 97.6 (s, C^i/C_6H_4), 97.9 (s, C^i/C_6H_4), 102.0 (d, $^1J_{CP}$ = 9.1 Hz, Ph_2PC≡C), 102.5 (d, $^1J_{CP}$ = 8.7 Hz, Ph_2PC≡C), 109.0 (s, C^i/C_6H_4), 110.5 (d, $^2J_{CP}$ = 23.4 Hz, FcC≡CP), 110.9 (s, C^i/C_6H_4), 128.3 (d, $^3J_{CP}$ = 10.9 Hz, C^m/C_6H_5), 128.8 (d, $^3J_{CP}$ = 10.9 Hz, C^m/C_6H_5), 130.1 (d, $^1J_{CP}$ = 53.4 Hz, C^i/C_6H_5), 130.8 (d, $^4J_{CP}$ = 2.3 Hz, C^p/C_6H_5), 130.9 (d, $^4J_{CP}$ = 2.2 Hz, C^p/C_6H_5), 132.3 (d, $^1J_{CP}$ = 52.5 Hz, C^i/C_6H_5), 133.0 (d, $^2J_{CP}$ = 10.8 Hz, C^o/C_6H_5), 134.4 (d, $^2J_{CP}$ = 10.5 Hz, C^o/C_6H_5). $^{31}P\{^1H\}$ NMR (101.249 MHz, $CDCl_3$, δ): −44.8 (s, FcC≡CP), −0.8 (s, Ph_2PC≡C). HRMS (ESI-TOF) $C_{70}H_{71}FeP_3Ru_3Cl_6$ [M]$^+$ *m/z*: calcd.: 1578.9370, found: 1578.9253; [M–RuCl$_2$(η^6-*p*-cymene)]$^+$ *m/z*: calcd.: 1270.9866, found: 1270.9751.

2.6. General procedure for the catalytic reactions

122 mg (1.0 mmol) of benzoic acid, 77 mg (0.5 mmol) of acenaphthene (internal standard) and 1.0 mol% (based in Ru) of the respective catalyst (**3a**–**3e** or **10**) were dissolved in 15 mL of chloro benzene. After addition of 0.87 mL (84 mg, 1.5 mmol) of propargyl alcohol the reaction mixture was stirred at 80 °C and samples (0.5 mL) were taken in periods of 1 h. The samples were dried in vacuum and the conversions were determined by ^1H NMR spectroscopy.

2.7. Crystal structure determination

The crystal and intensity collection data for **3b**, **3c**, and **10** are summarized in Table 1. The data were collected with an Oxford Gemini S diffractometer with graphite monochromatized Mo Kα radiation (λ = 0.71073 Å) at 100 K. The structures were solved by direct methods using SHELXS-97 [25] and refined by full-matrix least-square procedures on F^2 using SHELXL-97 [26]. All *non*-hydrogen atoms were refined anisotropically and a riding model was employed in the refinement of the hydrogen atom positions.

3. Results and discussion

The (ethynylferrocenyl)phosphino ruthenium(II) complexes (FcC≡C)R$_2$P(RuCl$_2$(η^6-*p*-cymene)) (**3a**, R = C_6H_5; **3b**, R = 2-$CH_3C_6H_4$; **3c**, R = $^cC_4H_3O$; **3d**, R = *t*-Bu; **3e**, R = $^cC_6H_{11}$; *p*-cymene = 1-$^iC_3H_7$-4-CH_3-C_6H_4; Fc = Fe(η^5-C_5H_4)(η^5-C_5H_5)) were synthesized by treatment of P(C≡CFc)R$_2$ (**1a**–**1e**) [20] with 0.5 equiv. of dimeric

Table 1
Crystal and intensity collection data for **3b**, **3c** and **10**.

	3b	3c	10
Formula weight	847.81	680.32	3681.84
Chemical formula	$C_{37}H_{38}Cl_5FePRu$	$C_{30}H_{29}Cl_2FeO_2PRu$	$C_{145}H_{149}Cl_{25}Fe_2P_6Ru_6$
Crystal system	triclinic	triclinic	triclinic
Space group	$P\bar{1}$	$P\bar{1}$	$P\bar{1}$
a (Å)	10.1745(3)	9.7028(12)	12.1915(5)
b (Å)	12.3193(4)	10.8658(6)	14.3215(5)
c (Å)	15.2195(4)	13.8545(7)	25.1595(10)
α (°)	81.358	74.085	96.926
β (°)	87.010	78.058	103.679
γ (°)	69.003	85.551	96.136
V (Å^3)	1760.76(9)	1373.9(2)	4195.2(3)
ρ_{calc} (g cm^{-3})	1.599	1.644	1.457
F(000)	860	688	1850
Crystal dimensions (mm)	0.3 × 0.3 × 0.3	0.2 × 0.2 × 0.1	0.2 × 0.2 × 0.1
Z	2	2	1
Maximum and minimum transmission	1.00000, 0.95682	1.00000, 0.94896	1.00000, 0.93550
Absorption coefficient (λ, mm^{-1})	1.293	1.357	1.192
Scan range (°)	3.03–25.00	2.78–25.00	3.27–25.00
Index ranges	$-8 \leqslant h \leqslant 12$ $-14 \leqslant k \leqslant 14$ $-18 \leqslant l \leqslant 18$	$-11 \leqslant h \leqslant 11$ $-12 \leqslant k \leqslant 12$ $-16 \leqslant l \leqslant 16$	$-14 \leqslant h \leqslant 14$ $-17 \leqslant k \leqslant 16$ $-29 \leqslant l \leqslant 29$
Total reflections	14838	12978	33943
Unique reflections	6158	4798	14712
R_{int}	0.0234	0.0234	0.0234
Data/restraints/para-meters	6158/0/406	4798/0/334	14712/66/868
Goodness-of-fit (GOF) on F^2	1.043	1.107	1.059
R_1[a], wR_2[a] [I 2σ(I)]	0.0508, 0.1249	0.0200, 0.0508	0.0527, 0.1430
R_1[a], wR_2[a] (all data)	0.0622, 0.1298	0.0252, 0.0526	0.0616, 0.1494
Largest differences in peak and hole peak in final Fourier map (e Å^{-3})	1.821, −1.155	0.450, −0.391	2.737, −1.691

[a] $R_1 = [\sum(||F_o| - |F_c||)/\sum|F_o|]$; $wR_2 = [\sum(w(F_o^2 - F_c^2)^2)/\sum(wF_o^4)]^{1/2}$; $S = [\sum w(F_o^2 - F_c^2)^2]/(n-p)^{1/2}$. n = number of reflections, p = parameters used.

$[RuCl_2(\eta^6\text{-}p\text{-cymene})]_2$ (**2**) in dichloromethane at ambient temperature (Reaction 1). After appropriate work-up, compounds **3a**–**3e** could be isolated as orange solid materials which are stable towards air and moisture for months. They dissolve in common organic solvents including dichloromethane, chloroform and tetrahydrofuran, while in diethyl ether, *n*-hexane and toluene they are not soluble.

chlorophosphine **7** failed due to its high reactivity and hence it was used in the synthesis of **9** without additional purification (Section 2). Addition of **7** to LiC≡CFc (**8**) in diethyl ether at low temperature gave by concomitant precipitation of LiCl red P(C≡CFc)(C≡CPPh$_2$)$_2$ (**9**) in moderate yield. Treatment of **9** with **2** produced (RuCl$_2$(η^6-*p*-cymene))(FcC≡C)P(C≡CPPh$_2$(RuCl$_2$(η^6-*p*-cymene))$_2$ (**10**). In heterometallic Ru$_3$Fe **10** the building blocks FcC≡C, C≡CPPh$_2$(RuCl$_2$(η^6-*p*-cymene) and RuCl$_2$(η^6-*p*-cymene) give rise to coordination number 4 at phosphorus.

Newly synthesized organometallic compounds **3**, **9** and **10** have been identified by elemental analysis, IR and NMR (^{1}H, ^{13}C{^{1}H}, ^{31}P{^{1}H}) spectroscopy. ESI TOF mass-spectrometry and single crystal X-ray structure analysis of **3b**, **3c** and **10** were additionally carried out. However, all complexes show the tendency to enclose solvent molecules which, even after 2–3 days in vacuum, could not be completely removed. These solvents include chloroform, dichloromethane and diethyl ether, whereas dichloromethane is able to displace the other solvents.

The IR spectra of **3**, **9** and **10** show very characteristic absorptions for the FcC≡C and Ph$_2$PC≡C alkynyl units in the expected region, i.e. at 2151 cm^{-1} ($\nu_{C\equiv CPPh2}$) and 2175 ($\nu_{C\equiv CFc}$) for **9** as well as 2155 cm^{-1} ($\nu_{C\equiv CPPh2}$) and 2179 ($\nu_{C\equiv CFc}$) for **10**. Upon coordination of the phosphorus atom in **1** and **9** to the 16-valence electron complex fragment RuCl$_2$(η^6-*p*-cymene) (formation of **3** and **10**) a small shift of the ferrocenyl acetylide and the phosphine alkynyl stretching frequencies to higher wavenumbers is induced, whereby the ferrocenyl-bonded C≡C triple bond is more affected (i.e. **1c**, $\nu_{C\equiv C}$ = 2153 [20]; **3c**, $\nu_{C\equiv C}$ = 2159 cm^{-1}; Section 2). As consequence thereof, IR spectroscopy is suited to monitor the progress of the reactions.

In the ^{13}C{^{1}H} NMR spectra the alkynyl groups create two (**3**) or four (**9** and **10**) exceptional resonance signals of which the phosphorus- (73–80 ppm, $^1J_{PC}$ = 13–127 Hz) and the ferrocenyl-bonded acetylide carbon atoms (107–110 ppm, $^2J_{PC}$ = 4–23 Hz) in **3a**–**3e** and **10** appear as doublets (Section 2). Complexation of the phosphorus atom in **1** and **9** to a RuCl$_2$(η^6-*p*-cymene)-fragment induces a shift of the phosphorus atom signal to lower field, which is characteristic in phosphorus transition metal chemistry [18]. While the coupling patterns in **1**, **3** and **10** are as expected (Section 2), compound **9** possesses a more complex signal splitting which is attributed to the increased number of phosphorus atoms present. Through the formation of a dative phosphorus–ruthenium bond in **10** the $^2J_{PC}$ coupling constant diminishes and hence is not anymore detectable in the spectrum. Also a shift of the *p*-cymene carbon atoms is observed when going from *non*-complexed to the coordinated species (Section 2). In **10** a set of two cymene units in the ratio of 2:1 is visible due to their different chemical environ-

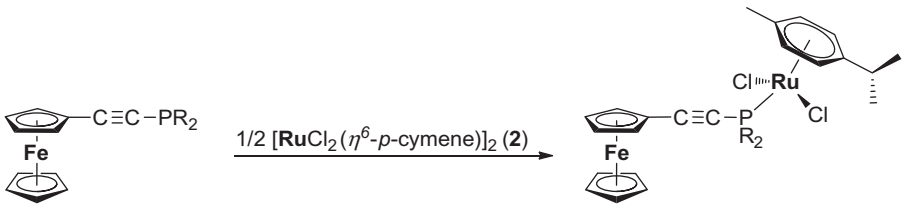

(1)

1 **3a - e**

Tetrametallic **10** was prepared applying the consecutive synthesis sequence shown in Scheme 1 of which the first three steps could be carried out in a one-pot procedure. Attempts to isolate

ments of which the signal of the inner phosphorus-bonded ruthenium dichloro *p*-cymene moiety is found at lower magnetic field. Notable in the spectrum of **10** is the observation of three signal sets

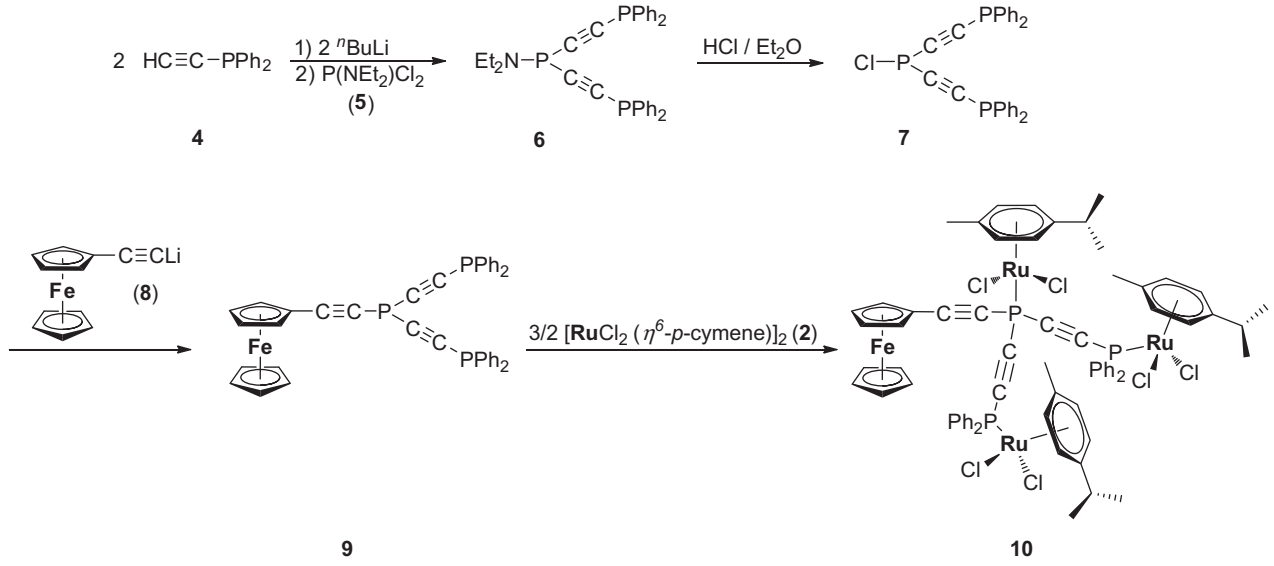

Scheme 1. Consecutive synthesis of tetrametallic **10**.

for the *iso*-propyl groups which can be explained by hindered rotation. The same behavior is found for the diphenylphosphino building blocks (Section 2).

As might have been expected, the ^{1}H NMR spectra of **3**, **9** and **10** consist of distinctive signal patterns as typical for the ferrocenyl and *p*-cymene units, respectively (Section 2).

A more expressive method than IR spectroscopy to verify the progress of the reaction is $^{31}P\{^{1}H\}$ NMR spectroscopy. A significant shift to lower field is observed upon coordination of the phosphines **3** and **9** to ruthenium (i.e. **1c**, −83.4 [20]; **3c**, −26.0 ppm, Section 2). Peculiar for **9** is the detection of a triplet at −88.2 (FcC≡CP) and a doublet at -32.7 (C≡CPPh$_2$) with $^{3}J_{PP}$ = 4.8 Hz, while in **10** this coupling diminishes.

The structures of **3b**, **3c**, and **10** in the solid state were determined by single X-ray diffraction studies confirming the half-sandwich configuration about the ruthenium(II) center and the tetrahedral environment at phosphorus. Single crystals of **3b** and **3c** could be grown from a saturated chloroform solution at ambient temperature, while crystals of **10** were accessible by slow diffusion of *n*-hexane into a saturated dichloromethane-chloroform solution (1:1, *v*:*v*) containing **10** at 25 °C. It was found that all molecules crystallize in the triclinic space group $P\bar{1}$. The molecular structures of **3b** and **3c** are shown in Fig. 1, Fig. 2 displays tetrametallic **10**. Geometric details of **3b** and **3c** are listed in Table 2, while the ones of **10** are summarized in the caption of Fig. 2. The crystallographic and refinement data of all compounds can be found in Table 1 (Section 2). Bond distances (Å), angles (°) and torsion angles (°) of the ethynylferrocenyl and *p*-cymene units are as expected and similar to those reported for closely related organometallic compounds [19–21,27].

Compounds **3b** and **3c** are set-up by the ferrocenylethynyl unit, the two organic groups R and the ruthenium dichloro *p*-cymene moiety at phosphorus (Fig. 1). For **3b** and **3c**, respectively, the bond angles around phosphorus P1 range from 108–123 ° and those around Ru1 from 84–95° (Table 2) indicating a characteristic "piano-stool" geometry (Fig. 1). The carbon–carbon triple bond distances C11–C12 are 1.198(8) (**3b**) and 1.204(3) (**3c**) Å, which is typical for this type of bonding [20,21,27]. The P1–C11–C12 and C11–C12–C6 units are with 178.8(5)° and 178.1(6)° (**3b**) as well as 170.91(18)° and 177.5(2)° (**3c**) essentially linear. The two ferrocenyl cyclopentadienyl rings in molecule **3c** are in a nearly eclipsed conformation (3.1°), whereas in complex **3b** both cyclopentadienyl rings are with 22.5° about in the middle between the fully eclipsed (0°) and the fully staggered (36°) conformation. The D1–Fe1 and D2–Fe1 separations are between 1.634–1.675 Å (D1 = centroid of C_5H_5, D2 = centroid of C_5H_4) and are similar to those of related compounds [20,21,27].

The key structural data of **10** (Fig. 2) confirm the half-sandwich structure about Ru1, Ru2 and Ru3. The coordination number around P1–P3 is four and along with the appropriate bond lengths and angles a "piano-stool" geometry is setup (Fig. 2). Mentionable are the distances Ru1–P1 (2.2772(12) Å, Ru2–P2 (2.3309(13) Å) and Ru3–P3 (2.3185(12) Å) proving, as expected, the stronger binding of the RuCl$_2$(η^6-cymene) unit by P1 explainable by the lower σ-donor capability compared with the respective alkynyl phosphine moieties [20,27]. All other bond distances and angles agree well with those building blocks reported for similar compounds [19–21,27].

The application of **3a**–**3e** and **10** in the homogeneous ruthenium-catalyzed addition of benzoic acid to propargyl alcohol for the synthesis of β-oxopropyl benzoate was studied as model system (Reaction 2).

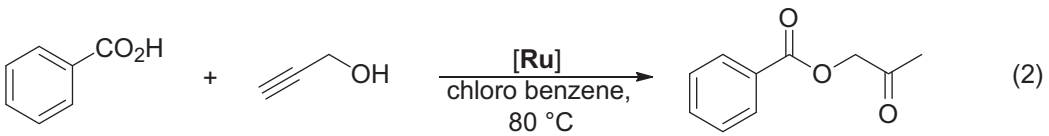

(2)

[Ru] = 3a - 3c, 10

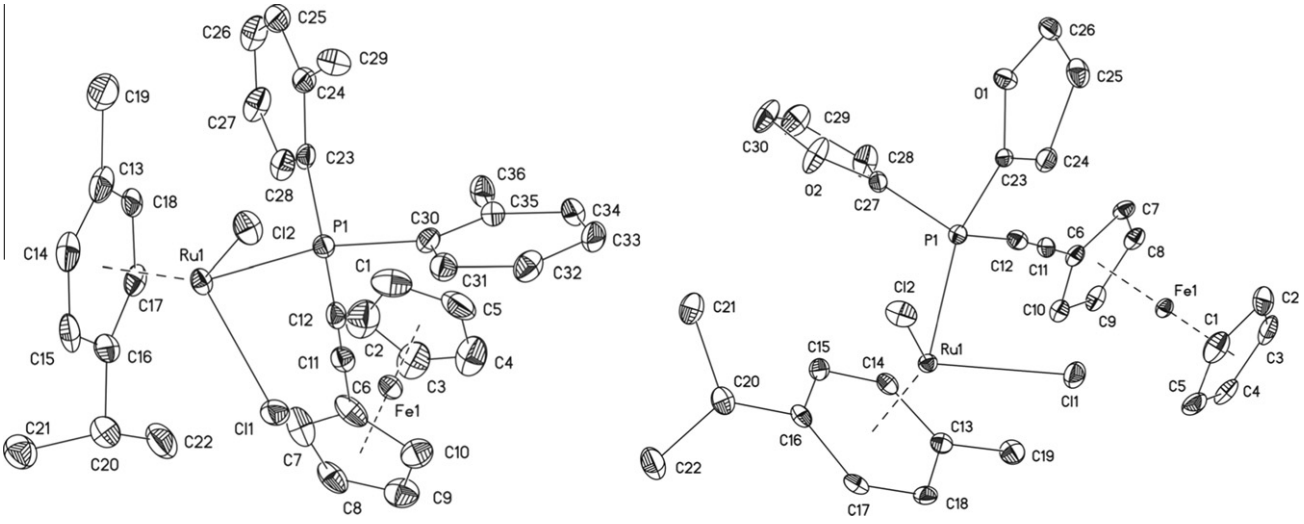

Fig. 1. ORTEP diagram (50% probability level) of the molecular structures of **3b** (left) and **3c** (right) with the atom numbering scheme. (Hydrogen atoms and chloroform as packing solvent of **3b** are omitted for clarity.)

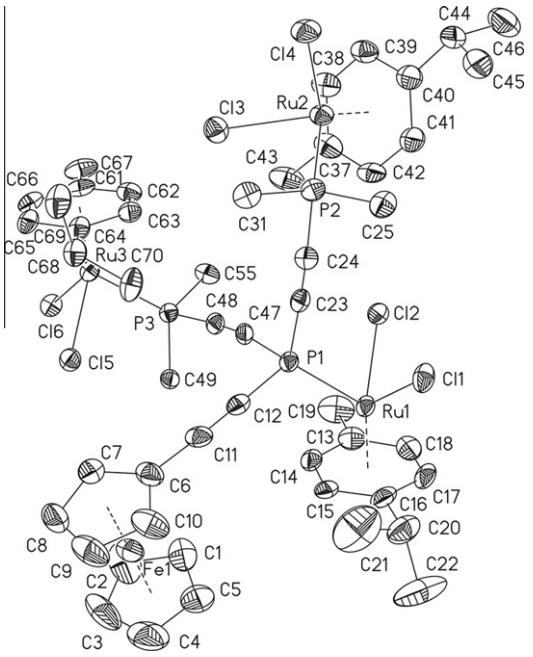

Fig. 2. ORTEP diagram (50% probability level) of the molecular structure of **10** with the atom numbering scheme. (Hydrogen atoms, packing solvent molecules and the phenyl groups (except the *ipso*-carbon atoms) are omitted for clarity.) Selected bond distances (Å), angles (°) and torsion angles (°): Fe1–D1 = 1.661, Fe1–D2 = 1.630, Ru1–D3 = 1.699, Ru2–D4 = 1.703, Ru3–D5 = 1.702, C11–C12 = 1.205(7), C23–C24 = 1.196(7), C47–C48 = 1.205(7), Ru1–Cl1 = 2.3995(12), Ru1–Cl2 = 2.4095(13), Ru1–P1 = 2.2772(12), Ru2–Cl3 = 2.4072(13), Ru2–Cl4 = 2.4171(13), Ru2–P2 = 2.3309(13), Ru3–Cl5 = 2.4077(12), Ru3–Cl6 = 2.4068(12), Ru3–P3 = 2.3185(12), P1–C12 = 1.742(5), P1–C23 = 1.764(5), P1–C47 = 1.758(5), P2–C24 = 1.770(5), P2–C25 = 1.831(5), P2–C31 = 1.822(5), P3–C48 = 1.763(5), P3–C49 = 1.829(5), P3–C55 = 1.826(5); D1–Fe1–D2 = 179.6, P1–C12–C11 = 170.1(5), P1–C23–C24 = 177.7(5), P1–C47–C48 = 170.3(4), C6–C11–C12 = 177.8(6), P2–C24–C23 = 175.9(4), P3–C48–C47 = 173.8(4); P1–C12–C11–C6 = -71(16), P1–C23–C24–P2 = -96(13), P1–C47–C48–P3 = 73(5). Standard uncertainties of the last significant digit(s) are shown in parenthesis. D1 = denotes the centroid of C_5H_5; D2 = denotes the centroid of C_5H_4, D3–D5 = denotes the centroids of C_6H_4.

Table 2
Selected bond lengths (Å), bond angles and torsion angles (°) for **3b** and **3c**.[a]

	3b	**3c**
Ru1–P1	2.3799(13)	2.3035(5)
Ru1–Cl1	2.4118(13)	2.4137(5)
Ru1–Cl2	2.4069(13)	2.4121(6)
P1–C12	1.764(6)	1.754(2)
P1–C23	1.831(5)	1.790(2)
P1–C27		1.804(2)
P1–C30	1.839(5)	
C11–C12	1.198(8)	1.204(3)
O1–C23		1.383(2)
O1–C26		1.362(2)
O2–C27		1.368(2)
O2–C30		1.371(3)
D1–Fe1[b]	1.634	1.640
D2–Fe1[b]	1.675	1.646
D3–Ru1[b]	1.706	1.696
Cl1–Ru1–Cl2	87.93(5)	88.29(2)
Cl1–Ru1–P1	84.06(5)	85.891(18)
Cl2–Ru1–P1	95.62(4)	91.442(19)
Ru1–P1–C12	108.98(17)	111.60(6)
Ru1–P1–C23	109.27(16)	119.87(6)
Ru1–P1–C27		116.38(6)
Ru1–P1–C30	123.96(18)	
P1–C12–C11	178.8(5)	170.91(18)
C12–C11–C6	178.1(6)	177.5(2)
C26–O1–C23		105.78(15)
C27–O2–C30		106.50(16)
D1–Fe1–D2[b]	178.1	179.6
P1–C12–C11–C6	−115(24)	21(6)
P1–C23–C24–C29	12.4(7)	
P1–C30–C35–C36	−1.1(8)	
Ru1–P1–C12–C11		69.7(11)
Ru1–P1–C23–O1		−167.51(11)
Ru1–P1–C27–O2		68.11(16)

[a] Standard uncertainties of the last significant digit(s) are shown in parenthesis.
[b] D1 denotes the centroid of C_5H_5 at Fe1; D2 denotes the centroid of C_5H_4 at Fe1; D3 denotes the centroid of C_6H_4 at Ru1.

Various ruthenium complexes featuring different electron-rich or electron-poor (ferrocenylethynyl)phosphino entities were screened in order to identify factors that may influence the catalytic activity and productivity. The donor capacity of the phosphines can be quantified by measuring the $^1J(^{31}P–^{77}Se)$ coupling constant of the appropriate seleno phosphines. Results thereof were previously published [20] indicating that phosphine **3c** possesses the weakest σ donor ability whereat the aliphatic phosphines **3d**, **e** show the best σ donor ability [20].

After screening different solvents, temperatures and catalyst concentrations we chose as best suited reaction conditions a

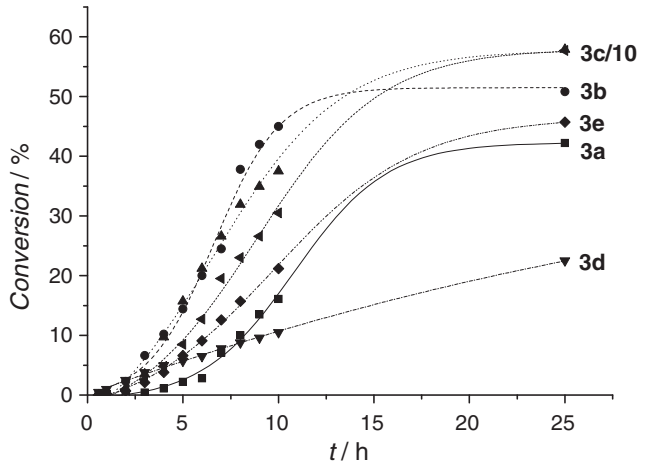

Fig. 3. Reaction profiles for catalysts **3a**–**3e** and **10** for the reaction of benzoic acid with propargyl alcohol to give β-oxopropyl benzoate (Reaction 2, catalyst loading 1.0 mol% based on Ru, 80 °C, chlorobenzene). Conversions equal ^{1}H NMR spectroscopic yields and are based on benzoic acid.

temperature of 80 °C, a concentration of 1.0 mol% and chloro benzene as solvent. However, in contrast to well-established systems [1a,9], below 80 °C no catalytic activity was observed. As best solvent chloro benzene was found which benefits from the high polarity and hence better solubility when compared to the commonly used solvent toluene [28]. The results of the catalytic investigations are summarized in Fig. 3.

From Fig. 3 it can be seen that under the reaction conditions mentioned above all complexes are catalytically active in the formation of β-oxo propyl benzoate in moderate to good yields. The most active catalyst is **3b** which shows a conversion of 45% within 10 h. Somewhat less active is furyl-substituted **3c** but shows the highest productivity (conversion 58%) after 25 h of all complexes **3a**–**3e**. Nevertheless, the lowest conversion (42%) within the series of aromatic/heteroaromatic phosphines is observed for the phenyl derivative **3a**. In addition, this phosphine needs a longer induction period of ca. 5 h to form the catalytically active species which might be responsible for the poor performance and low yield. Comparing the aromatic with the aliphatic phosphine substituents it is obvious that more electron-rich systems **3d** and **3e** are less active and only show productivities of 46% (**3e**) or 23% (**3d**) after 25 h (Fig. 3). However, due to the long reaction times necessary, all catalysts suffer from a loss of activity, which can be attributed to gradually decomposition of the catalyst during the course of the reaction. Nevertheless, no formation of "ruthenium black" which indicates the formation of ruthenium particles could be observed.

Also from Fig. 3 it can be seen that tetrametallic **10** with its three ruthenium(II) centers shows a significantly higher productivity than **3a** featuring only one ruthenium dichloro *p*-cymene building block. Furthermore, no induction period is observable. This phenomenon can most probably be ascribed to synergistic and cooperative effects between the appropriate transition metals which improves the catalytic activity with increasing number of active centers present in one molecule, i.e. dendritic carbene–palladium complexes [29], phosphino palladium-functionalized PAMAM dendrimers [30,31] and carbosilane dendrimers with end-grafted NCN pincer-nickel(II) groups [32]. Further examples include metallo-enzymes [33] and metal oxide supported catalysts [34].

Compared to $[RuCl_2(\eta^6\text{-}p\text{-cymene})(PR_3)]$ (R = Ph, Me) [1a] with basic phosphines and $[RuCl_2(\eta^6\text{-}p\text{-cymene})]_2/P(^cC_4H_3O)_3$ [9] with its electron-poor phosphine we could not find a general trend concerning basicity or steric factors under reaction conditions used by us (Fig. 3). We believe that it is a combination of both issues, whereas electron-poor ligands at the phosphorus atom are best suited, which is achieved by the introduction of an ethynylferrocenyl functionality. Moderate electron-rich species are only effective catalysts, when they possess at the same time bulky ligands, e.g. *ortho*-tolyl groups (Fig. 3). Also, some of our systems need longer reaction times and therefore, suffer from deactivation due to decomposition of the active species. Finally, it must be noted that, however, our catalysts only work at 80 °C, which differs from literature known species described by, for example, Dixneuf et al. [1] or Goossen et al. [9].

4. Conclusions

In this work, we presented the synthesis of novel heterobimetallic dinuclear and tetranuclear complexes of type $(FcC{\equiv}C)R_2P\text{-}(RuCl_2(\eta^6\text{-}p\text{-cymene}))$ (R = C_6H_5, 2-$CH_3C_6H_4$, $^cC_4H_3O$, *t*-Bu, $^cC_6H_{11}$; *p*-cymene = 1-$^iC_3H_7$-4-CH_3-C_6H_4; Fc = $Fe(\eta^5\text{-}C_5H_4)(\eta^5\text{-}C_5H_5)$) and $(RuCl_2(\eta^6\text{-}p\text{-cymene}))(FcC{\equiv}C)\text{-}P(C{\equiv}CPPh_2(RuCl_2(\eta^6\text{-}p\text{-cymene})))_2$, respectively. All molecules were used as catalysts in the formation of β-oxopropyl benzoate by treatment of propargyl alcohol with benzoic acid. All complexes show a catalytic activity with moderate to good conversions (23–58%). However, neither electronic properties nor steric factors alone are responsible for the catalytic performance, which differs from statements recently made [1,9]. We believe that it is more or less a combination of both criteria, whereas electron-poor ligands R are best suited. Moderate electron-rich species are only effective catalysts, when they possess bulky ligands.

Acknowledgements

We are grateful to the Deutsche Forschungsgemeinschaft and the Fonds der Chemischen Industrie for financial support.

References

[1] (a) D. Devanne, C. Ruppin, P.H. Dixneuf, J. Org. Chem. 53 (1988) 925;
(b) C. Bruneau, P.H. Dixneuf, Angew. Chem., Int. Ed. 45 (2006) 2176.
[2] (a) C. Bruneau, Z. Kabouche, M. Neveux, B. Seiller, P.H. Dixneuf, Inorg. Chim. Acta 222 (1994) 155;
(b) M. Neveux, B. Seiller, F. Hagedorn, C. Bruneau, P.H. Dixneuf, J. Organomet. Chem. 451 (1993) 133.
[3] V. Cadierno, J. Francos, J. Gimeno, Green Chem. 12 (2010) 135.
[4] D.W. Hansen Jr., R. Pappo, R.B. Garland, J. Org. Chem. 53 (1988) 4244.
[5] P. Yates, R.S. Grewal, P.C. Hayes, J.F. Sawyer, Can. J. Chem. 66 (1988) 2805.
[6] S. Costin, N.P. Rath, E.B. Bauer, Adv. Synth. Catal. 350 (2008) 2414.
[7] A.J. Fry, D. Herr, Tetrahedron Lett. 19 (1978) 1721.
[8] M.A. Ashraf, M.A. Jones, N.E. Kelly, A. Mullaney, J.S. Snaith, I. Williams, Tetrahedron Lett. 44 (2003) 3151.
[9] L.J. Goossen, J. Paetzold, D. Koley, Chem. Comm. (2003) 706.
[10] A.D. Cort, J. Org. Chem. 56 (1991) 6708.
[11] R.C. Cambie, R.C. Hayward, J.L. Jurlina, P.S. Rutledge, P.D. Woodgate, J. Chem. Soc., Perkin Trans. 1 (1978) 126.
[12] S. Torii, T. Inokuchi, S. Misima, T. Kobayashi, J. Org. Chem. 45 (1980) 2731.
[13] S. Stavber, B. Sket, B. Zajc, M. Zupan, Tetrahedron 45 (1989) 6003.
[14] M.M. Salunkhe, A.R. Sande, A.S. Kanade, P.P. Wadgaonkarb, Synth. Commun. 27 (1997) 2885.
[15] M. Arfan Ashraf, A.G. Russell, C.W. Wharton, J.S. Snaith, Tetrahedron 63 (2007) 586.
[16] M. Rotem, Y. Shvo, Organometallics 2 (1983) 1689.
[17] (a) C. Ruppin, P.H. Dixneuf, Tetrahedron Lett. 27 (1986) 6323;
(b) C. Ruppin, P.H. Dixneuf, S. Lecolier, Tetrahedron Lett. 29 (1988) 5365;
(c) K. Philippot, D. Devanne, P.H. Dixneuf, J. Chem. Soc., Chem. Commun. (1990) 1199.
[18] R. Packheiser, H. Lang, Eur. J. Inorg. Chem. (2007) 3786.
[19] P. Stepnicka, J. Demel, J. Cejka, J. Molec. Catal. A: Chem. 224 (2004) 161.
[20] B. Milde, D. Schaarschmidt, P. Ecorchard, H. Lang, J. Organomet. Chem., in press, doi:10.1016/j.jorganchem.2012.01.017.
[21] T. Baumgartner, M. Fiege, F. Pontzen, R. Arteaga-Müller, Organometallics 25 (2006) 5657.
[22] Vi. Huc, A. Balueva, R.-M. Sebastian, A.-M. Caminade, J.-P. Majoral, Synthesis 5 (2000) 726.

[23] S.-Z. Luo, Y.-M. Li, Z.-Z. Chen, H. Abe, L.-P. Cui, H. Nakanishi, X.-R. Qin, Y.-F. Zhao, Lett. Pept. Sci. 10 (2003) 57.
[24] S. Suravajjala, J.R. Polam, L.C. Porter, J. Organomet. Chem. 461 (1993) 201.
[25] G.M. Sheldrick, Acta Crystallogr., Sect. A 46 (1990) 467.
[26] G.M. Sheldrick, SHELXL-97, Program for Crystal Structure Refinement, University of Göttingen, 1997.
[27] A. Jakob, B. Milde, P. Ecorchard, C. Schreiner, H. Lang, J. Organomet. Chem. 693 (2008) 3821.
[28] C. Schreiner, Ph.D. Thesis, TU Chemnitz, Germany, 2010.
[29] V. Hornillos, J. Guerra, A. de Cozar, P. Prieto, S. Merino, M.A. Maestro, E. Diez-Barra, J. Tejeda, Dalton Trans. 40 (2011) 4095.
[30] M.T. Reetz, G. Lohmer, R. Schwickardi, Angew. Chem., Int. Ed. Engl. 36 (1997) 1526.
[31] S. Dietrich, A. Nicolai, H. Lang, J. Organomet. Chem. 696 (2011) 739.
[32] J.W.J. Kapen, A.W. van der Made, J.C. de Wilde, P.W.N.M. van Leeuwen, P. Wijkens, D.M. Grove, G. van Koten, Nature 372 (1994) 659.
[33] E.K. van den Beuken, B.L. Feringa, Tetrahedron 54 (1998) 12985.
[34] B. Coq, F. Figueras, Coord. Chem. Rev. 178–180 (1998) 1753.
[35] V. Cadierno, J. Francos, J. Gimeno, Organometallics 30 (2011) 852.